Bulletin of Engineering Geology and the Environment (2021) 80:4379–4387
https://doi.org/10.1007/s10064-021-02253-y

ORIGINAL PAPER

Judgement of rapid drawdown conditions in slope stability analysis

Xiao-ping Hou[1] · Sheng-hong Chen[2] · Isam Shahrour[3]

Received: 5 June 2020 / Accepted: 17 April 2021 / Published online: 20 April 2021

Abstract

The rapid drawdown of reservoir may have a significant impact on the stability of adjacent slopes. In order to avoid potential risks, it is important to calculate the change of slope safety factor prior to the reservoir operation. The finite element method is used to analyze the transient seepage during drawdown, and then the pore water pressures are introduced into the stability computation based on limit equilibrium to obtain the transient safety factor. Computations show that for slopes with a specific geometry, the safety factor ratio depends on the parameters $K/(S_y v)$ (where K is the permeability coefficient, v is the drawdown speed, and S_y is the specific yield) and $c'/(\gamma H \tan \phi')$ (where c' and ϕ' are the effective cohesion and friction angle, γ is the soil unit weight, and H is the slope height). By considering a wide range of $K/(S_y v)$ and $c'/(\gamma H \tan \phi')$ values and different slope geometries, the percent reduction in critical safety factor of slope during drawdown relative to that during steady-state seepage is obtained. The drawdown condition that causes a large percent reduction in safety factor is judged as a rapid drawdown, and the opposite is a slow drawdown, which does not affect the slope design. This paper presents a series of charts for engineers and designers to judge rapid and slow drawdown conditions. Before the reservoir operation, the appropriate drawdown speed is selected according to the charts to ensure a slow drawdown for adjacent slope, while in the slope stabilization design, only the rapid drawdown stability analysis needs to be performed.

Keywords Slopes · Rapid drawdown · Transient seepage · Stability analysis · Safety factor

Introduction

Engineering practice shows that the reservoir drawdown conditions may have an important impact on the stability of adjacent slopes (International Committee on Large Dams 1980; Lawrence Von Thun 1985; Paronuzzi et al. 2013; Sun et al. 2017). Indeed, during a rapid reservoir drawdown, the pore water in soil cannot drain at the speed of the reservoir drawdown. Consequently, the phreatic surface in the slope could become higher than the water level in the reservoir, resulting in transient seepage flowing out of the slope. The pore water pressure generated by transient seepage reduces the shear strength along the potential sliding surface, which probably destabilizes the slope. In practical engineering, precautions should be taken to prevent slope instability due to a rapid drawdown (Abramson et al. 2002).

Previous studies on the impact of the reservoir drawdown speed on slope stability classified the drawdown conditions into rapid drawdown and slow drawdown (Liu et al. 2005; Berilgen 2007; Sun et al. 2017, 2018). Since rapid drawdown is detrimental to the stability of the slope, it must be taken into account in the stabilization design of dam and reservoir bank slopes (US Army Corps of Engineers 2003). The ratio $K/(S_y v)$ was commonly used in the previous studies as the indicator for judging rapid drawdown (Mao 2003), where K is the soil permeability coefficient (unit: m/d), v is the speed of water-level drawdown in the reservoir (unit: m/d), and S_y is the specific yield, also known as drainage porosity, which is a ratio less than or equal to the effective porosity, indicating the ratio of the volume of water that an unconfined aquifer will release from storage by gravity to the total volume of saturated aquifer. Experiments show that when $K/(S_y v) \leq 0.1$, the lowering of the phreatic surface is very small relative to the water-level drawdown, so the drawdown is judged to be rapid; when $K/(S_y v) > 10$, the

✉ Xiao-ping Hou
xiaopingyatou@163.com

[1] Key Laboratory of Ministry of Education for Agricultural Soil and Water Engineering in Arid and Semiarid Areas, Northwest A&F University, Yangling 712100, China

[2] State Key Laboratory of Water Resources and Hydropower Engineering Science, Wuhan University, Wuhan 430072, China

[3] Laboratoire Génie Civil et géo-Environnement, Université Lille 1, 59655 Villeneuve d'Ascq, France

phreatic surface drops almost synchronously with the water level; therefore, it is judged as slow drawdown (Liu et al. 2005). The US Army Corps of Engineers (1970) presented the chart for determining the height of the phreatic surface at the impervious core wall at the end of drawdown by using the indicator $K/(S_y v)$. S-H. Chen (2015) concluded that when $K/(S_y v) < 0.1$, rapid drawdown should be considered and the phreatic surface before drawdown can be employed to estimate the pore water pressure in the stability analysis; when $K/(S_y v) > 60$, the drawdown is slow and rapid drawdown may be ignored in the stability analysis; when $0.1 < K/(S_y v) < 60$, the drawdown speed is moderate and analysis of transient seepage is needed to determine the phreatic surface during drawdown. The indicator values for judging the speed of drawdown would be different if the slope structure and drainage conditions are different.

Ideally, the speed of the water-level drawdown in the reservoir should be small enough to allow the phreatic surface to closely follow the water level and ensure slope safety. However, in response to sudden rainstorms, rapid drainage from the reservoir is inevitable. It is helpful to avoid risks by calculating the change of slope safety factor with the drawdown of water level before the operation of the reservoir. NR. Morgenstern (1963) investigated the change of the safety factor of soil slope during rapid drawdown using the limit equilibrium method, and proposed a series of safety factor charts for practicing engineers to utilize. It should be noted that these charts are based on the assumption that the drawdown is very fast and no drainage occurs in soil, thus the term "sudden" drawdown. This assumption is also adopted by PA. Lane and Griffiths (2000) and NA. Hammouri et al. (2008). Viratjandr and Michalowski (2006) examined the change of the safety factor as the water level drops when the water level in the reservoir and the phreatic surface in the slope are at different relative positions using the limit analysis method. Although the safety factor can be estimated from the charts for the specific water levels in the reservoir and in the slope, the true rate of the drainage in soil is dependent on the permeability coefficient K, the drawdown speed v, and the specific yield S_y. Accurate analysis of slope stability requires simulation of transient seepage. MM. Berilgen (2007) presented a numerical method for coupling transient seepage and deformation analyses including consolidation. This method was used to compare the changes of the safety factor with the drawdown of water level at two drawdown speeds, permeability coefficients, and slope heights. The results demonstrate that when the soil permeability coefficient is low and the drawdown speed is rapid, the slope may fail, especially the high slope that does not possess a high degree of safety prior to the drawdown.

At present, the stabilization design of dam and reservoir bank slopes considers both long-term steady-state seepage condition and rapid drawdown condition (US Army Corps of Engineers 2003; National Reform and Development Commission of China 2006). The rapid drawdown stability analysis generally adopts the assumption of no drainage within soil. If the assumption appears to be excessively conservative and the sudden drawdown analysis controls the slope design, simulation of the relative drainage process (i.e., transient seepage) in soil could be performed. The main work of this paper is to systematically investigate the change of safety factor of the slope subjected to transient seepage under different drawdown conditions. In evaluating the stability of the slope, the percent reduction in the minimum (critical) safety factor during the drawdown relative to that during the steady-state seepage is used as the basis. If the drawdown causes the safety factor to reduce by a large percentage, it may threaten the stability of the slope and is therefore judged as a rapid drawdown condition. Contrarily, it is identified to be a slow drawdown condition that does not affect the slope safety. By considering the ranges of drawdown speeds, soil material properties, and slope geometries commonly encountered in engineering practice, a series of charts for engineers and designers to judge the rapid and slow drawdown conditions are presented. Before the operation of the reservoir, the appropriate drawdown speed can be selected from the charts to ensure a slow drawdown for the adjacent slope, while in the slope stabilization design, only the stability analysis with respect to the rapid drawdown needs to be performed.

Basic assumptions and methods used in the investigation

Basic assumptions

(1) The investigation covers slopes built with different soils (clayed soil or sandy soil). The slopes have different heights H, top widths L, and inclinations m ($m = \cot \beta$, where β is the inclination angle of the slope), as shown in Fig. 1. These slopes are seated on a rigid and impermeable base.

(2) An analysis of reservoir drawdown is made from the situation where the reservoir is full and the soil is fully saturated to the situation where the reservoir is empty but the soil is partly or fully saturated. As illustrated in Fig. 1, in the initial situation, the water-level height is equal to the height of the slope (H), while in the final situation, the water-level height is zero.

(3) The water level in the reservoir drops at a constant speed v.

(4) It is assumed that the soil is homogeneous, isotropic, and incompressible, and is saturated below the phreatic surface.

(5) Consider that the lateral boundary of the transient seepage in the soil is a vertical wall. In the dam, it represents the impervious core wall, and in the bank slope of the

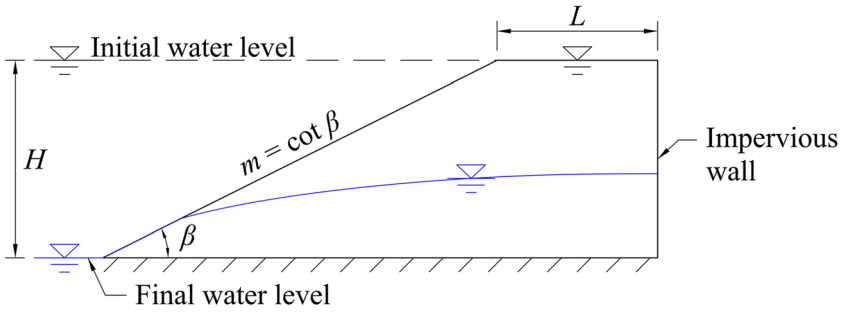

Fig. 1 The drawdown problem in homogeneous slopes

reservoir, it is the outermost boundary affected by the drawdown.

(6) Assume that the critical sliding surface is circular and intersects the slope face.

Uncoupled transient seepage and slope stability analyses

The finite element method is used to simulate the transient seepage, and then the obtained pore water pressure is introduced into the stability analysis based on limit equilibrium to compute the transient safety factor of the slope during the water-level drawdown. The two analyses are performed in a completely uncoupled manner. Despite recent advances in coupled seepage and deformation analyses (Berilgen 2007; Pinyol et al. 2008), this method usually comes at the cost of computation time and complicated numerical implementation. The purpose of this investigation is to ascertain the impact of the water-level drawdown on the slope safety factor, and the deformation and consolidation of the medium are not the focus of study. Therefore, the uncoupled analysis method with both simplicity and effectiveness is selected.

Simulation of transient seepage using finite element

Based on the above assumptions and considering Darcy's law and continuity equation, the differential equation of transient seepage in the soil is expressed by

$$\frac{\partial}{\partial x}\left(K_x\frac{\partial h}{\partial x}\right)+\frac{\partial}{\partial y}\left(K_y\frac{\partial h}{\partial y}\right)=S_s\frac{\partial h}{\partial t} \tag{1}$$

where $h = y + u/\gamma_w$ is the total head, y is the elevation, u is the pore water pressure, γ_w is the unit weight of water, K_x and K_y are the permeability coefficients in x and y directions respectively, and S_s is the elastic specific storage. For homogeneous, isotropic, and incompressible soils, $K_x = K_y = K$ and $S_s = 0$. Then, Eq. (1) is simplified as the Laplace equation, i.e., $\partial^2 h/\partial x^2 + \partial^2 h/\partial y^2 = 0$.

Equation (1) is subject to the initial condition

$$h = H \quad \text{at } t = 0 \tag{2}$$

and the boundary conditions illustrated in Fig. 2

$$h = H - H_D(t) \quad \text{on } \Gamma_1 \tag{3}$$

$$\frac{\partial h}{\partial n} = 0 \quad \text{on } \Gamma_2 \tag{4}$$

$$h = \xi(x,t) \quad \text{on PS} \tag{5}$$

$$K\left(\frac{\partial h}{\partial x}\frac{\partial \xi}{\partial x}-\frac{\partial h}{\partial y}\right)=S_y\frac{\partial h}{\partial t} \quad \text{on PS} \tag{6}$$

$$h = y \quad \text{on SF} \tag{7}$$

where H_D is the height of the water-level drawdown, n points to the normal direction of the boundary, and Γ_1 and Γ_2 are respectively the first and second types of boundaries. In Eqs. (5) and (6), ξ is introduced to represent the elevation of the phreatic surface (PS). The phreatic surface has the property that water flow cannot cross it, so in Eq. (6), the flow velocity normal to the phreatic surface must be equal to the velocity of

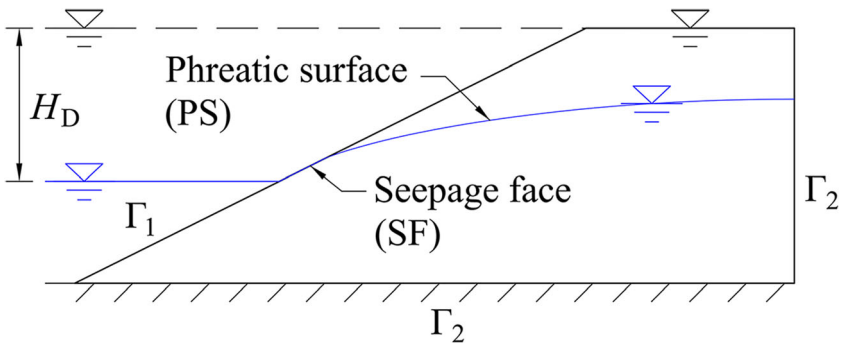

Fig. 2 Four types of boundaries in the seepage area

the phreatic surface normal to itself. On the seepage face (SF), water is in contact with air and thus the total head equals the elevation in Eq. (7).

The finite element equation of transient seepage is derived from the variational analysis of Eqs. (1)–(7), which has the following form:

$$K[A]\{h\} + S_y[B]\left\{\frac{\partial h}{\partial t}\right\} = 0 \tag{8}$$

where

$$A_{ij} = \sum_{element}\iint\left(\frac{\partial N_i}{\partial x}\frac{\partial N_j}{\partial x} + \frac{\partial N_i}{\partial y}\frac{\partial N_j}{\partial y}\right)dxdy$$

$$B_{ij} = \sum_{element}\int -N_i N_j\sqrt{1+\partial\xi/\partial x}dx$$

and N is the shape function in the element.

When calculating Eq. (8), a suitable difference scheme, such as implicit difference, is employed to replace the time derivative in Eq. (8) to lead to

$$\left(\Delta tK/S_y[A]^{t_0} + [B]^{t_0}\right)\{h\}^{t_0+\Delta t} = [B]^{t_0}\{h\}^{t_0} \tag{9}$$

The time domain is divided into multiple discrete time steps Δt, and the total head at the new time is calculated step by step from the total head at the initial time. In the process of calculation, an iterative algorithm is adopted to determine the shifting phreatic surface and seepage face, and the total head on the boundary Γ_1 must be equal to its prescribed value ($H - H_D$). This algorithm has been implemented in a computer program developed by X-P. Hou et al. (2015) for simulating unsteady seepage with a free surface, and will not be repeated here.

Obviously, it can be concluded from Eq. (9) that the total head at different times depends on the ratio $\Delta tK/S_y$ and the corresponding boundary value ($H - H_D$). Since

$$\Delta t = \frac{H_D{}^{t_0+\Delta t} - H_D{}^{t_0}}{v} \tag{10}$$

the transient seepage results when the water level drops to any elevation remain unchanged as long as the $K/(S_y v)$ value is constant. This is why $K/(S_y v)$ can be used as the indicator to estimate the height of the phreatic surface in the slope.

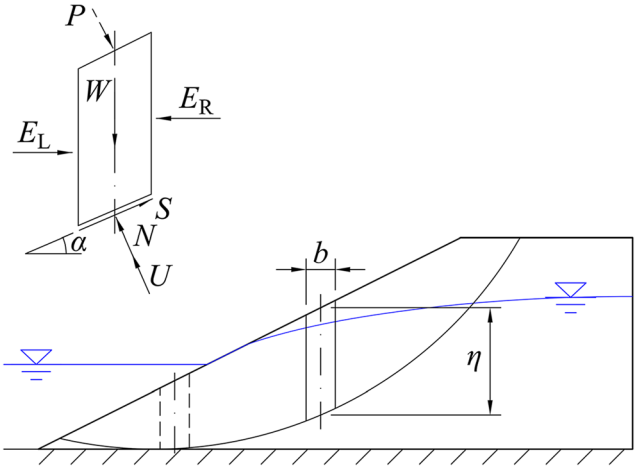

Fig. 3 Forces acting on a slice inside the sliding body enclosed by a circular surface in submerged slope

Analysis of slope stability using limit equilibrium

The circular sliding of the slope is analyzed by the Bishop simplified method (Bishop 1955). Figure 3 illustrates the forces acting on a slice inside the sliding body enclosed by the circular surface, including the weight W of the slice with the width b and height η, the horizontal normal forces E_L and E_R between the slices, and the normal force N, shear force S, and uplift force U due to pore water pressure at the bottom of the slice. If the top of the slice is submerged below the water level, it is also subjected to the water load P. For any trial sliding surface, the safety factor F_s is equal to the ratio of the total resisting shear forces to the total driving shear forces along the sliding surface.

In order to simplify the computational formula of the safety factor, the replacement method proposed by Z-Y. Chen (2003) is used to replace the case where the slope is submerged (in Fig. 3) with the case of non-submerged slope shown in Fig. 4. Two treatments are needed to maintain the equivalence of the forces: (a) The weight W of the slice is replaced by W minus the weight of water with the same volume as the slice below the water level ($W - W_w$); (b) the uplift force U due to pore water pressure at the bottom of the slice is replaced by the uplift force due to excess pore water pressure ($U - U_w$). Moreover, the water load P generated by the water level in the reservoir is no longer considered. Finally, the formula for computing F_s is

$$F_s = \frac{\sum\left\{c'b + [(W-W_w)-(U-U_w)cos\alpha]\tan\phi'\right\}/\left[\cos\alpha\left(1 + tan\alpha tan\phi'/F_s\right)\right]}{\sum(W-W_w)\sin\alpha} \tag{11}$$

where c' and ϕ' are the effective cohesion and effective friction angle respectively, and α is the angle between the tangent to the center of the slice base and the horizontal.

Substituting the expressions $W = \gamma b\eta$, $W_w = \gamma_w b\eta_w$, $U = ub/\cos\alpha$, and $U_w = \gamma_w\eta_w b/\cos\alpha$ into Eq. (11), and expressing the linear dimensions as ratios of the slope height H, Eq. (11) is

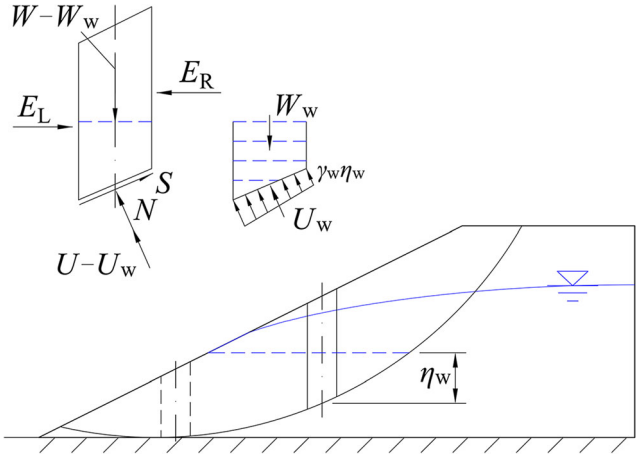

Fig. 4 Forces acting on the slice after replacing the case of submerged slope with the non-submerged case

converted into

$$\frac{F_s}{\tan\phi'} = \frac{\sum\left[\frac{c'}{\gamma H\tan\phi'} + \left(\frac{\eta}{H} - \frac{u}{\gamma H}\right)\right] \Big/ \left[\cos\alpha\left(1 + tan\alpha \cdot \frac{tan\phi'}{F_s}\right)\right]}{\sum\left(\frac{\eta}{H} - \frac{\gamma_w}{\gamma}\frac{\eta_w}{H}\right)\sin\alpha} \quad (12)$$

where γ is the unit weight of soil, u is the pore water pressure at the center of the slice base, and η_w is the height of the slice below the water level. The software product STAB developed by Z-Y. Chen (2003) is employed to compute the safety factor. An optimization method (Chen 1992) has been implemented in STAB to determine the critical circular sliding surface, across which the safety factor reaches the minimum.

It can be seen from Eq. (12) that for slopes with a specific geometry, the safety factor ratio $F_s/\tan\phi'$ is related to $c'/(\gamma H\tan\phi')$ and $u/(\gamma H)$. Since the pore water pressure depends only on $K/(S_y v)$, the safety factor ratio during the drawdown differs according to the values of $K/(S_y v)$ and $c'/(\gamma H\tan\phi')$.

Material parameters

The representative values of permeability coefficient and specific yield are selected based on the field and laboratory measurements for various types of geological materials summarized by Singhal and Gupta 2010). As listed in Table 1, the minimum value K/S_y = 0.05 m/d represents a weak pervious soil with K = 0.0005 m/d and S_y = 0.01 (typically, a clayed soil); and the maximum value K/S_y = 500 m/d represents a strong pervious soil with K = 50 m/d and S_y = 0.1 (typically, a gravel soil). Assuming that the water-level drawdown speed v is equal to 0.5 m/d, the $K/(S_y v)$ value varies from 0.1 to 1000.

The value of the parameter $c'/(\gamma H\tan\phi')$ is set between 0 and 1, as shown in Table 1. These values represent most of the cases encountered in drawdown problems. Relatively large values of $c'/(\gamma H\tan\phi')$ are characteristics of low slopes built using soil with a small friction angle, e.g., $c'/(\gamma H\tan\phi')$ = 0.82 when c' = 30 kPa, ϕ' = 10°, H = 10 m, and γ = 20.8 kN/m^3. The smaller values of $c'/(\gamma H\tan\phi')$ describe higher slopes built using soil with the lower cohesion but larger friction angle, e.g., $c'/(\gamma H\tan\phi')$ = 0.03 when c' = 10 kPa, ϕ' = 25°, H = 40 m, and γ = 18 kN/m^3. Given that its most critical failure mechanism approaches sliding along a planar surface, the c' = 0 (i.e., non-cohesive) property is not involved in this investigation. The use of parameters $K/(S_y v)$ and $c'/(\gamma H\tan\phi')$ to simplify the presentation of the data has been discussed in detail in the previous section.

Table 1 Values of the parameters used in the investigation

Parameters	Values					
K/S_y (m/d)	0.05	0.5	5	50	500	
$K/(S_y v)$	0.1	1	10	100	1000	
$c'/(\gamma H\tan\phi')$	0.03	0.14	0.27	0.55	0.82	1

Results and discussion

Lowering of phreatic surface during water-level drawdown

The distribution of phreatic surfaces in the slope (L/H = 1.2 and m = 2) under different water levels when $K/(S_y v)$ = 0.1, 1, 10, 100, and 1000 is presented in Fig. 5. It can be seen from Fig. 5 that the smaller the $K/(S_y v)$ value, the more obviously the lowering of the phreatic surface lags behind the water-level drawdown. For $K/(S_y v)$ = 0.1, the phreatic surface remains at a high position at the end of the drawdown. In this case, the assumption made by NR. Morgenstern (1963) is reasonable that no drainage occurs in soil during drawdown. However, as the value of $K/(S_y v)$ increases, the speed of lowering of the phreatic surface is accelerated. When $K/(S_y v)$ = 1000, the phreatic surface and the water level drop almost synchronously, and the transient seepage condition corresponding to any intermediate water level is close to the long-term steady-state seepage condition, under which the phreatic surface has stabilized at the new water level.

Change of safety factor during water-level drawdown

The transient safety factors of the slope (L/H = 1.2 and m = 2) are obtained by introducing the pore water pressure distributions under different water levels into limit equilibrium analyses. Figure 6 shows the change of the slope safety factor ratio $F_s/\tan\phi'$ with the drawdown of water level when $K/(S_y v)$ = 0.1, 1, 10, 100, and 1000 and $c'/(\gamma H\tan\phi')$ = 0.14. It can be seen from Fig. 6 that $F_s/\tan\phi'$ reduces with the increase of the

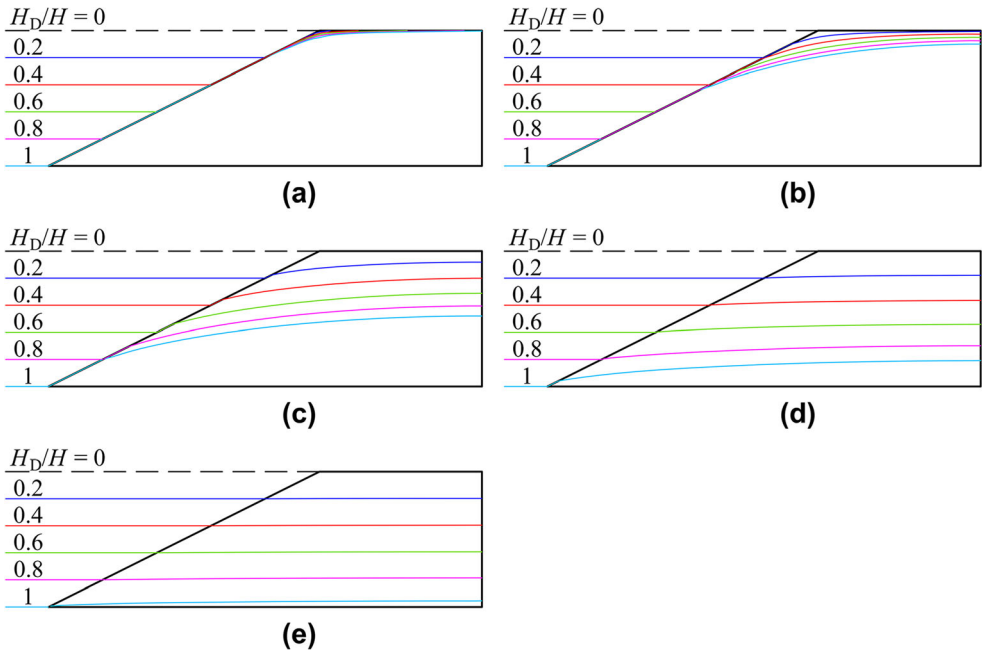

Fig. 5 Lowering of the phreatic surface in the slope (L/H = 1.2, m=2) with water-level drawdown when $K/(S_y v)$ has different values. **a** 0.1. **b** 1. **c** 10. **d** 100. **e** 1000

drawdown ratio. It reaches the minimum value when H_D/H = 0.7–1.0. Near the end of the drawdown, the increased shear strength due to reduced pore water pressure has a greater impact than the weakened stabilizing action due to the drawdown of water level, so the safety factor is increased. For large values of $K/(S_y v)$ ($K/(S_y v) \geq 100$), the minimum $F_s/\tan\phi'$ occurs at the ratio of the water-level drawdown height to its original height equal to 0.7. The relationship between $F_s/\tan\phi'$ and H_D/H under steady-state seepage is presented in Fig. 6 for comparison. It is found that the change curve of the safety factor ratio for $K/(S_y v)$ = 1000 coincides with the steady-state seepage condition.

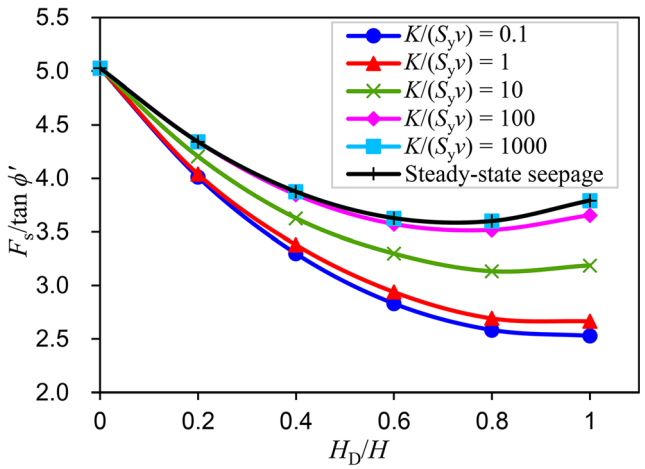

Fig. 6 Change of the safety factor ratio of the slope (L/H = 1.2, m=2) with water-level drawdown when $K/(S_y v)$ = 0.1, 1, 10, 100, and 1000, and $c'/(\gamma H\tan\phi')$ = 0.14

Allowable reduction range of safety factor during drawdown

In fact, when considering the drawdown condition for the slope, a temporarily reduced safety factor is usually allowed, which is different from normal working condition (long-term steady-state seepage). As shown in Table 2, in the DL/T 5353-2006 "Design specification for slope of hydropower and water conservancy project" formulated by the National Reform and Development Commission of China (2006), the design safety factor of the slope under the rapid drawdown (1.00–1.15) can be 0–0.2 lower than that under the long-term steady-state seepage (1.00–1.25). The specific reduction range varies according to the grade of the slope and its initial safety factor. Similarly, in the EM 1110-2-1902 "Engineering and design: Slope stability" developed by the US Army Corps of Engineers (2003), the minimum design safety factor corresponding to the rapid drawdown (1.1) is 0.4 lower than the steady-state seepage (1.5). It is easy to understand that if the slope safety factor reduces beyond the allowable range during drawdown, the drawdown condition will control the slope stabilization design. On the contrary, the steady-state seepage condition plays a decisive role in the design of the slope. The data in Table 2 shows that as long as the initial safety factor of the slope is greater than 1.10, the reduction of 5% in the safety factor caused by the drawdown is still within the allowable range. In this study, this condition is judged as a slow drawdown, and the opposite is a rapid drawdown.

Charts for judging rapid drawdown conditions

By investigating the changes of the safety factor of slopes with different material parameters and geometries when

Table 2 The specified safety factors of slopes in design specifications

Design specifications	Slopes	Analysis conditions	
		Normal working (long-term steady-state seepage)	Rapid drawdown
DL/T 5353-2006[a]	Grade I slope at reservoir area	1.15–1.25	1.05–1.15
	Grade II slope at reservoir area	1.05–1.15	1.05–1.10
	Grade III slope at reservoir area	1.00–1.10	1.00–1.05
EM 1110-2-1902	New earth and rock-fill dams	1.5	1.1–1.3

[a] The slopes at the reservoir area are divided into three grades according to engineering grade, slope position, service life, and harm extent of a failure, which are assigned different design safety factors respectively

subjected to different speed drawdowns, the percent reduction in the critical safety factor during the drawdown relative to that during the steady-state seepage can be obtained. Then, the drawdown conditions are classified according to the allowable reduction range of the safety factor during drawdown. Figure 7 shows a series of charts for judging the conditions of rapid and slow drawdown for slopes with different geometries. They are L/H = 0, 0.4, 0.8, 1.2, and 1.6, and m = 1, 1.5, 2, 2.5, and 3. The high and steep slopes are characteristics of the bank slopes of the reservoir, and

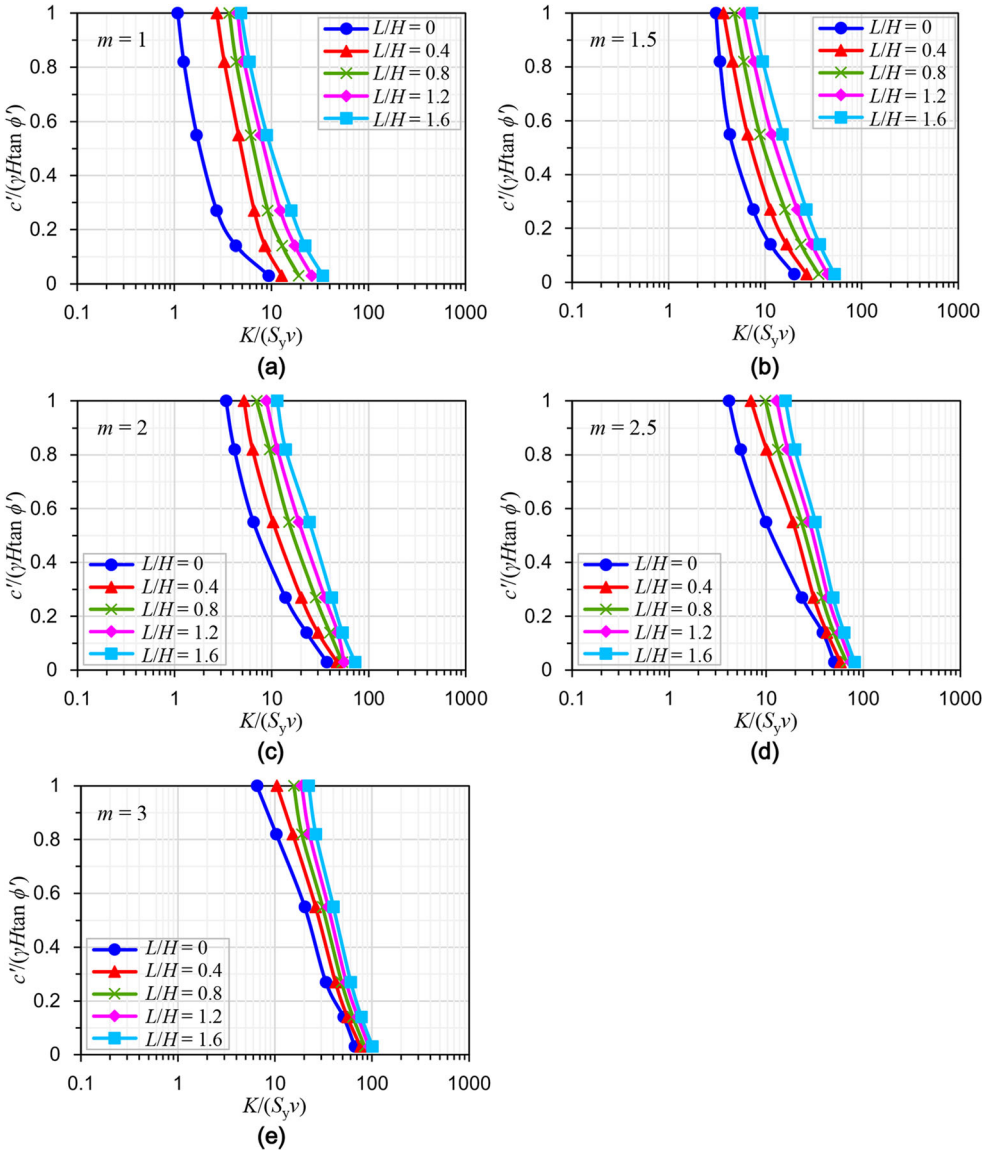

Fig. 7 Charts for judging rapid drawdown conditions for slopes with different geometries. **a** m = 1. **b** m = 1.5. **c** m = 2. **d** m = 2.5. **e** m = 3

the low and gentle slopes may be the upstream slope of the earth dams. Each demarcation line in the charts divides the $K/(S_y v)$–$c'/(\gamma H \tan \phi')$ space into two areas: the left area—rapid drawdown and the right area—slow drawdown. The critical safety factor of the slope under rapid (or slow) drawdown reduces by more than (or less than) 5% compared to that under steady-state seepage.

It can be seen from Fig. 7 that as L/H and m increase, the demarcation line between rapid and slow drawdown moves to the right, that is, the rapid drawdown area increasingly expands. Due to the poor drainage conditions of the low and gentle slopes, the safety factor is significantly reduced during the drawdown, so it is more likely to form a rapid drawdown. However, this does not mean that the low and gentle slopes under the same drawdown events (the same $K/(S_y v)$ and $c'/(\gamma H \tan \phi')$ values) tend to be more dangerous than the high and steep slopes, but that their stability is strongly influenced by the drawdown. It is more important for engineers to know well the change rather than the normal value of the safety factor when the slope is subjected to the drawdown of the reservoir. Furthermore, Fig. 7 reveals the rule that when the value of $c'/(\gamma H \tan \phi')$ is small, the $K/(S_y v)$ threshold for judging rapid and slow drawdown is relatively large. It should be noted that the change in pore water pressure caused by the drawdown affects only the frictional force related to ϕ' rather than the cohesive force related to c'. Therefore, when the frictional force plays a major role in the total shear resistance, the slope safety factor changes greatly with the drawdown of water level, and the probability of a rapid drawdown condition is high.

Conclusion

This paper proposes a criterion for judging the conditions of rapid drawdown in slope stability analysis. The criterion is based on the percent reduction in the critical safety factor during the drawdown relative to that during the steady-state seepage. Considering the transient seepage and potential circular sliding, the changes of the slope safety factor under different drawdown conditions are investigated in detail. Through the analysis of the transient seepage finite element equation, the reason why the phreatic surface and pore water pressure distributions in the slope are controlled by the $K/(S_y v)$ value is explained. Then, the simplified Bishop computational formula for the safety factor of submerged slope is established by the replacement method. This formula demonstrates that for slopes with a specific geometry, the safety factor ratio $F_s/\tan \phi'$ depends on the parameter $c'/(\gamma H \tan \phi')$ and the pore water pressure expression $u/(\gamma H)$, which is only related to $K/(S_y v)$. The use of $K/(S_y v)$ and $c'/(\gamma H \tan \phi')$ facilitates the creation of generic charts. By considering a wide range of $K/(S_y v)$ and $c'/(\gamma H \tan \phi')$ values as well as different slope geometries, a series of charts for engineers and designers to judge the rapid drawdown conditions for the slopes are finally produced.

Before the operation of the reservoir, the values of $K/(S_y v)$ and $c'/(\gamma H \tan \phi')$ are first determined according to the proposed drawdown speed and the material parameters and geometry of the slope. Then, the charts presented in this paper are visited to judge whether the speed is rapid or slow to the slope. For the rapid drawdown, the speed needs to be further reduced to ensure that the slope works under the condition of slow drawdown. In the slope stabilization design, the maximum drawdown speed of the reservoir is used to calculate the value of $K/(S_y v)$, and then it is checked from the charts whether it leads to a rapid drawdown. The stability analysis with respect to the rapid drawdown controls the stabilization design of the slope, while the slow drawdown analysis can be omitted because it does not change the original stability status of the slope. This paper provides practical guidance for quickly determining if a drawdown analysis is needed in the slope stabilization design.

It should be noted that the allowable reduction range of the safety factor during the drawdown is associated with the importance of the slope, the engineering purpose, and the initial safety factor. Theoretically, if the slope has a higher safety factor against steady-state seepage, the allowable range for the reduction in the safety factor due to the drawdown is larger. This paper adopts the Chinese design specification, and identifies the condition that the safety factor reduces by more than 5% during the drawdown as a rapid drawdown. If other design specifications (e.g., USA) are adopted, the judgment criterion for rapid drawdown will change accordingly. The methods and results in this paper can be used as references for making other charts. In addition, this investigation does not involve slopes built with non-cohesive soil, because their most dangerous failure mechanism is close to sliding along the plane.

Code availability The source code of the STAB program used for slope stability analysis in this study is available in the corresponding reference. The custom code used for transient seepage simulation in this study is currently not available, but the relevant numerical algorithms and reliability verification can be found in the corresponding reference.

Author contribution The study conception and design were contributed by Xiao-ping Hou and Sheng-hong Chen. Data collection, formal analysis, and investigation were performed by Xiao-ping Hou. The first draft of the manuscript was written by Xiao-ping Hou and all authors commented on previous versions of the manuscript. All authors read and approved the final manuscript.

Funding This research was supported by Scientific Startup Foundation for Doctors of Northwest A&F University (No. 2452018038).

Data Availability The data generated and used during the study has been presented in the figures and tables of the submitted article. More relevant data is available from the corresponding author by request (E-mail address: xiaopingyatou@163.com).

Declarations

Competing interests The authors declare no competing interests.

References

Abramson LW, Lee TS, Sharma S, Boyce GM (2002) Slope stability and stabilization methods. Wiley, New York

Berilgen MM (2007) Investigation of stability of slopes under drawdown conditions. Comput Geotech 34(2):81–91. https://doi.org/10.1016/j.compgeo.2006.10.004

Bishop AW (1955) The use of the slip circle in the stability analysis of slopes. Géotechnique 5(1):7–17. https://doi.org/10.1680/geot.1955.5.1.7

Chen Z-Y (1992) Random trials used in determining global minimum factors of safety of slopes. Can Geotech J 29(2):225–233. https://doi.org/10.1139/t92-026

Chen Z-Y (2003) Soil slope stability analysis: theory, methods and programs. China Water Power Press, Beijing [in Chinese]

Chen S-H (2015) Hydraulic structures. Springer Verlag, New York

Hammouri NA, Malkawi AIH, Yamin MMA (2008) Stability analysis of slopes using the finite element method and limiting equilibrium approach. Bull Eng Geol Environ 67(4):471–478. https://doi.org/10.1007/s10064-008-0156-z

Hou X-P, Xu Q, He J, Chen S-H (2015) Composite element algorithm for unsteady seepage in fractured rock masses. Chin J Rock Mech Eng 34(1):48–56 [in Chinese]

International Committee on Large Dams (1980) Deterioration of dams and reservoirs: examples and their analysis. Balkema, Rotterdam

Lane PA, Griffiths DV (2000) Assessment of stability of slopes under drawdown conditions. J Geotech Geoenviron Eng 126(5):443–450. https://doi.org/10.1061/(ASCE)1090-0241(2000)126:5(443)

Lawrence Von Thun J (1985) San Luis Dam upstream slide. Int Conf on Soil Mech Found Eng 11:2593–2598

Liu X-X, Xia Y-Y, Lian C, Zhang K-P (2005) Research on method of landslide stability valuation during sudden drawdown of reservoir level. Rock Soil Mech 26(9):1427–1431 [in Chinese]

Mao C-X (2003) Seepage computation analysis and control. China Water Power Press, Beijing [in Chinese]

Morgenstern NR (1963) Stability charts for earth slopes during rapid drawdown. Géotechnique 13:121–131. https://doi.org/10.1680/geot.1963.13.2.121

Paronuzzi P, Rigo E, Bolla A (2013) Influence of filling–drawdown cycles of the Vajont reservoir on Mt. Toc slope stability Geomorphology 191:75–93. https://doi.org/10.1016/j.geomorph.2013.03.004

Pinyol NM, Alonso EE, Olivella S (2008) Rapid drawdown in slopes and embankments. Water Resour Res 44, W00D03. https://doi.org/10.1029/2007WR006525

National Reform and Development Commission of China (2006) Design specification for slope of hydropower and water conservancy project, DL/T 5353-2006. Beijing

Singhal BBS, Gupta RP (2010) Applied hydrogeology of fractured rocks. Springer Verlag, New York

Sun G, Yang Y, Jiang W, Zheng H (2017) Effects of an increase in reservoir drawdown rate on bank slope stability: a case study at the Three Gorges Reservoir, China. Eng Geol 221:61–69. https://doi.org/10.1016/j.enggeo.2017.02.018

Sun G, Lin S, Jiang W, Yang Y (2018) A simplified solution for calculating the phreatic line and slope stability during a sudden drawdown of the reservoir water level. Geofluids. https://doi.org/10.1155/2018/1859285

US Army Corps of Engineers (1970) Engineering and design: stability of earth and rock-fill dams, EM 1110-2-1902. Washington, DC

US Army Corps of Engineers (2003) Engineering and design: slope stability, EM 1110-2-1902. Washington, DC

Viratjandr C, Michalowski RL (2006) Limit analysis of submerged slopes subjected to water drawdown. Can Geotech J 43(8):802–814. https://doi.org/10.1139/t06-042